Glucocorticoids target postnatal oligodendrocyte precursor cells to modulate adult hippocampal network plasticity and stress-induced behavior

Authors:

Lorenzo Mattioni[1,2*], Giulia Poggi[1,3*], Celine Gallagher[4*], Katrin Becker[3], Maja Papic[5], Jasmin Engbers[3], Maija-Kreetta Koskinen[6,7,] , Ali Abdollahzade[6,7], David Herzog[3], Leonardo Nardi[1], Andrea Conrad[8], Sarah Winterberg[9], Hans Schwarzbach[9], Jan Engelmann[3], Beat Lutz[8,10], Ari Waisman[5], Iiris Hovatta[6,7] , Thomas Mittmann[4], Michael J. Schmeisser[1,2], Marianne B Müller[2, 3,10*], Giulia Treccani[1,3,9*]

Affiliations:

1. Institute of Anatomy, University Medical Center of the Johannes Gutenberg-University Mainz, Mainz, Germany

2. Focus Program Translational Neurosciences, University Medical Center of the Johannes Gutenberg-University, Mainz, Germany

3. Department of Psychiatry and Psychotherapy, University Medical Center of the Johannes Gutenberg-University Mainz, Mainz, Germany

4. Institute of Physiology, University Medical Center of the Johannes Gutenberg-University, Mainz, Germany.

5. Institute for Molecular Medicine, University Medical Center of the Johannes Gutenberg-University Mainz, Mainz, Germany

6. SleepWell Research Program, Faculty of Medicine, University of Helsinki, Helsinki, Finland

7. Department of Psychology, Faculty of Medicine, University of Helsinki, Helsinki, Finland

8. Institute of Physiological Chemistry, University Medical Center of the Johannes Gutenberg University

9. Department of Systemic Neuroscience, Institute of Anatomy and Cell Biology, Philipps University, Marburg, Germany

10. Leibniz Institute for Resilience Research, Mainz, Germany

* indicates equal contributions

Corresponding author

Univ.-Prof Dr. Giulia Treccani

Department of Systemic Neuroscience

Institute of Anatomy and Cell Biology

University of Marburg

Robert-Koch-Straße 8

35032 Marburg, Germany

Tel. 06421-28 26507

Email: treccani@staff.uni-marburg.de

Keywords:NG2-glia, OPCs, glucocorticoid receptor, hippocampus, learning and memory, electrophysiology, non-canonical role of OPC

Abstract

Aversive early experiences affect brain development and enhance the risk of psychiatric disorders. Recent evidence has implicated oligodendrocyte precursor cells (OPCs) in the pathophysiology of stress-related diseases. Beside their myelination-dependent functions, OPCs are involved in the fine-tuning of neuronal activity and responding to environmental challenges. OPCs express the glucocorticoid receptor (GR) binding glucocorticoids (GCs) and are sensitive to aversive experiences. To decipher the role of early postnatal GCs on OPC maturation, neuronal network activity and adult behavior we conditionally deleted GR in postnatal OPCs. Such deletion resulted in a reduction of oligodendrocytes in the hippocampus, alteration of hippocampal network activity and impairment in the formation of memories in adulthood. Our findings reveal a novel role for postnatal GRs in modulating OPC maturation, neuronal network excitability and adult memory formation. This provides the first evidence for a dual role of GR signaling in both the canonical and non-canonical functions of OPCs.

Introduction

Early experiences, both positive and negative, are vital for brain development and play an essential role in building brain architecture after birth. Indeed, the human brain reaches full adult maturity well into the third decade of life[1]. This capitalizes on prolonged postnatal brain development, during which early life experiences configure and fine-tune brain networks. The latter mostly relies on experience-dependent synaptic pruning and myelination. While positive experiences have beneficial effects on such processes, exposure to early life adversity (ELA) during childhood is detrimental and has been linked to the risk of developing stress-related psychiatric disorders later in life[2]. ELA is common[3] and has the power to override the so-called stress-hyporesponsive period, which normally protects the postnatal brain from stress-induced surges in circulating corticosteroid hormones[4].

Importantly, different cell populations of the brain are endowed with glucocorticoids receptors (GRs), making them sensitive to physiological fluctuations, but also to stress-induced increase of glucocorticoids (GCs)[5]. One glial cell population that has been identified both clinically and preclinically as an emerging player in stress-related psychiatric disorders[6–9] are oligodendrocyte precursor cells (OPCs). OPCs express several markers, including the chondroitin sulfate proteoglycan 4 (CSPG4) or neuron-glial antigen 2 (NG2), and are therefore also referred to as NG2-glia[10,11]. They are homogeneously distributed throughout the CNS, both during development and adulthood, and they are highly responsive to external stimuli, including neuronal activity[12]. Through their canonical pathway, OPCs can give rise to myelinating oligodendrocytes. However, a large proportion of OPCs remain undifferentiated and surveys the surrounding extracellular environment[13]. These resident OPCs are thought to play a critical role in modulating and fine-tuning neuronal networks, through non-

canonical (and myelination independent) pathways[14–18] and are indeed integrated into the neuronal network via synapses with neighbouring neurons [19–21]. Mice exposed to maternal separation (a model of ELA) have an increased number of mature oligodendrocytes at postnatal day (P)15 and a reduction in OPCs as adults[22]. In post-mortem studies on individuals exposed to ELA, increased numbers of mature myelinating oligodendrocytes (OLs) and decreased numbers of OPCs, were found[23]. Taken together, these findings suggest enhanced maturation of OPCs as a result of their early exposure to excess GCs. Recently, we have shown that ELA not only alters the density of OPCs or OLs, but has a direct effect on the OPC gene expression patterns and their electrical properties, and that these effects are largely GR-dependent[24].

Intriguingly, OPCs, reactive to stress during the total lifespan[25–28] and express GRs in various grey and white matter areas of the brain[29,30], suggesting a physiological role of GC in OPC function and differentiation, both *in vivo* and *in vitro*[31].

Despite the converging evidence that GCs affect OPC properties, two striking gaps in knowledge remain: (1) What is the role of constitutive GR expression on the differentiation and proliferation of OPCs and their properties in modulating neuronal network activity? (2) do GR-physiologically prime OPCs to fine-tune behavior, in particular those behavioral phenotypes, typically observed in stress models and stress-related pathologies in humans?

To address these questions, we conditionally deleted GRs in OPCs in the first postnatal week, targeting the period when these cells reach their proliferative peak[32]. We analyzed the long-lasting effects of such manipulation on oligodendrocyte proliferation and differentiation dynamics, hippocampal neuronal network properties and ultimately complex behavior.

Results

Conditional deletion of glucocorticoid receptor in OPCs impairs lineage maturation, without affecting proliferation and morphology.

To investigate the role of an early cKO of GR on OPC differentiation, morphology, as well as behavioral phenotypes in adult mice, we generated an OPC-specific GR conditional knockout (cKO) mouse strain. We obtained the cKO mice by crossing the Ng2CreER^{T2} mice with Nr3c1$^{fl/fl}$ mice and inducing recombination by tamoxifen injection at postnatal day (PD) 2 and 4 (Fig. 1a, see Material and Method section for details). As previously reported[28,30], we confirmed by FACS analysis that GRs are expressed by the hippocampal and cortical OPCs and mature oligodendrocytes (OLs), with the OPCs having a higher concentration of GRs (Supplementary Fig. 1a, b). We then assessed the efficiency of GR deletion in OPCs by performing immunofluorescence (IF) staining in the dorsal hippocampus (Fig. 1b) and the dorsally located somatosensory cortex of the cKO and control littermates. Immunostaining revealed a significant decrease in the percentage of GR+ NG2+ Olig2+ OPCs in cKO mice in both the hippocampus (Fig. 1c, d) and cortex (Supplementary Fig. 2b). To confirm the specificity of GR deletion in OPCs, we performed co-staining of GR with several cell-specific markers, including Glial fibrillary acidic protein (GFAP) for astrocytes (Supplementary Fig. 3a-c), Ionized calcium binding adaptor molecule 1 (Iba1) for microglia (Supplementary Fig. 3d-f), NeuN for neurons (Supplementary Fig. 3g-i) and Platelet-derived growth factor receptor beta (PDGFRB) for pericytes (Supplementary Fig. 3j-k). We did not observe a reduction of GRs in any of these cell populations in cKO mice, either in the hippocampus or in the cortex.

We then asked whether the cKO of GR would affect the hippocampal density of OPCs and OLs, stained with NG2 and Aspartoacylase (ASPA, marker for mature myelinating OLs) respectively. We did not find significant changes in the density of OPCs (Fig. 1e, f) or in the density of mature OLs (Fig. 1g, h) in the hippocampus of cKO mice compared to littermate controls. These data were confirmed by FACS analysis, which showed no difference in the number of PDGFRA+ OPCs but a significant decrease in CNPase+ OL, both gated from the CD45-CD11b- global populations (Fig. 1k, l).

Since an imbalance in OPC and OL ratio may be a consequence of an alteration in OPC proliferation[33], we performed IF staining for Ki-67, a marker for cell proliferation, and PDGFRA, a marker for OPCs, and quantified the overall density of OPCs (PDGFRA+ cells), proliferative cells (Ki-67+ cells) and proliferative OPCs (PDGFRA+ Ki-67+ cells). The density of proliferative OPCs was comparable between cKO and littermate controls (Fig. 1i, j). A slightly different pattern was observed in the cortex. Indeed, while a reduction of OPCs density was observed when employing the NG2 marker (Supplementary Fig. 2c), no changes were observed in OL density (Supplementary Fig. 2d), nor in OPCs proliferation (Supplementary Fig. 2e) or in OPC density when using PDGFRA as a marker (Supplementary Fig. 2g). The absence of difference in the density of OPCs and OLs in the cortex was further validated by FACS analysis (Supplementary Fig. 2h-i).

Another fundamental feature of the OPCs is their morphological complexity, which allows for continuous and efficient surveillance of the surrounding environment. It drastically diminishes when OPCs undergo apoptosis or mature [13,26]. Critically, GR KO in OPCs did not influence the length and complexity of the cells, which had a similar total length of the filaments (Supplementary Fig. 4a, b) and similar filament arborization as shown in the Sholl analysis compared with the controls (Supplementary Fig. 4c).

This suggests that the loss of GR is unlikely to severely alter OPCs surveillance capabilities and, in line with the density readouts, does not lead to cell atrophy, as is observed for instance, in response to stressors prior to apoptosis[26].

To assess whether the reduction in mature oligodendrocyte density was reflected in an overall decrease of myelin-related proteins and/or in the alteration myelin structural features, we performed western blot (WB) analysis on hippocampal and cortical lysates from cKO and littermate control mice. However, we found no differences in the protein levels of MBP (all isoforms analyzed together), PLP[34], CNP, or ASPA in either the hippocampus or cortex in cKO and control mice (Supplementary Fig. 5 and 6). Furthermore, we performed 3D reconstruction and morphological analysis of the paranodes and nodes of Ranvier in Ctrl vs. cKO mice and found no differences between the groups (Supplementary Fig. 7).

Taken together these data demonstrate that loss of GR in OPCs in early life leads to a reduction of mature oligodendrocytes in the hippocampus during adulthood, potentially suggesting a brain region-specific alteration in maturation dynamics of the OL lineage.

Early conditional deletion of GR cKO in OPCs alters the excitability of the neuronal network in response to acute challenge later in life

To understand whether the deletion of GR in OPCs could impact on the function of the neuronal network, we performed electrophysiological multi-electrode array (MEA) recordings. The experiments were performed under control conditions and after the application of the GR agonist dexamethasone. This experimental condition mimicked *in vitro* the activation of the HPA axis and thus of the GR-related pathway. Horizontally-sectioned brain slices were placed on the MEA chip so that extracellular field excitatory

postsynaptic potentials (fEPSPs) along the Schaffer Collateral CA3 to CA1 pathway could be measured (Fig. 2a, for details see Materials and Methods). The evoked fEPSPs were recorded in the CA1 region and the maximum signal amplitudes plotted for both male and female adult mice (Fig. 2b-c). Male mice, whether control or cKO, did not show a differential response in terms of evoked field potential amplitude after dexamethasone application. Female control mice, however, showed a significantly increased evoked field potential amplitude for all stimulation inputs ranging from 2.5 – 5V when dexamethasone was applied (Fig. 2c), implying a change in postsynaptic AMPA-dependent mechanisms. Interestingly, the female cKO mice did not show this increase in response to dexamethasone application. The loss of this field potential amplitude increase in the NG2-specific GR cKO mice implies that this receptor is highly relevant for the acute stress response in female mice. Representative traces of the evoked fEPSPs before and after the 30-minute application of dexamethasone for male control (Fig. 2d (i-ii)), female control (Fig. 2d (iii-iv)), male cKO (Fig. 2e (i-ii)) and female cKO (Fig. 2e (iii-iv)) can be seen in Fig. 2. Importantly, sex-specific dichotomy in the evoked excitability experiments was also seen even before dexamethasone was applied. Male mice had a higher evoked hippocampal excitability at baseline, as seen by the significantly larger evoked responses for both wildtype and cKO males before dexamethasone application when compared to that of female mice (Supplementary Fig. 7).

In addition, paired-pulse stimulation recordings (PPR) were carried out to investigate whether dexamethasone application, mimicking acute stress exposure, induces synaptic facilitation/depression and/or changes in presynaptic mechanisms in the Schaffer collateral pathway. Dexamethasone application caused a significant increase in the PPR in the female control mice, while the effect in the male controls, was

significant but very small. Once again, this effect was lost in the cKO groups (Fig. 3a). Interestingly, this strongly reflects the significant changes seen in the evoked excitability experiments above (Fig. 2). When comparing the different groups before dexamethasone application, a trend for an overall slight difference between genotypes was detected by the two-way ANOVA (Fig. 3b, see Supplementary Table for the Statisitcs). Representative traces of the paired-pulse stimulation responses, with a 50ms interstimulus interval, can be seen for the male (Fig. 3c (i)) and female (Fig. 3c (ii)) control groups. No change in the amplitude of either the first or second paired-pulse stimulation response was in the male group after the application of dexamethasone (Fig. 3c (i)). In the case of the female control group, there was an increase in the amplitude of both the first and the second paired-pulse stimulation responses on the application of dexamethasone, with the second undergoing a relatively larger increase in amplitude (Fig. 3c ii). The first response is most likely associated with postsynaptic AMPAR-mediated mechanisms[35,36], similarly to the increased amplitudes from the I/O curve above (Fig. 2). The second response, however, is dependent on the level of presynaptic calcium influx which increases neurotransmitter release probability[37,38]. Taken together, these changes represent a synaptic facilitation, and the probability of neurotransmitter release by the second stimulation remains high (Fig. 3a).

No changes in the rate of spontaneous network activity were observed in the hippocampal slices of either sex or genotype after dexamethasone application (Supplementary Fig. 8). However, sex-specific dichotomy was again observed in the mean spontaneous spike frequency before dexamethasone was applied (Supplementary Fig. 8b), with the female mice, in general, having a higher mean spike frequency than male mice.

In conclusion, the exclusivity of these effects at a pre-and post-synaptic level to the female control mice is very intriguing and divulges an exquisite and fundamental sex-specific function of the NG2-cell specific GR, for both pre- and post-synaptic acute stress response and/or arousal-related mechanisms of the hippocampal Schaffer collateral pathway.

Postnatal deletion of GR in OPCs induces impairment in memory and aversive learning tasks but does not alter anxiety-relevant behavior or sociability in adulthood

Since changes in the ratio between OPCs and OLs and in the activity of neuronal network may have consequences on behavioral outcomes[22], we performed a battery of tests encompassing different behavioral domains in control littermate and cKO mice. We tested the mice from the less to the more aversive tests and performed the open field (OF) test to assess locomotor activity, the novel object recognition test (NORT) for cognitive performance, the three-chamber sociability test for sociability, the dark-light box (LB) for anxiety-relevant behavior and at the end the two-way active avoidance test (TWA) for aversive learning. When mice were tested in the OF arena, they did not display any differences among genotypes in locomotor activity (Fig. 4a), neither in the time they spent in the more anxiogenic part of the arena, the center, (Fig. 4b) nor at the rim (or periphery of the arena) (Fig. 4c). Interestingly the female mice of both genotypes spent significantly more time in the less anxiogenic part of the OF arena (See Supplementary Table for the Statistics), the rim. We then assessed cognitive performance in the NORT test. We first checked that in the training phase of the test, the animals, randomly assigned to an identical object pair, did not show a preference for one of the two identical object positions (Fig. 4d). After an inter-trial time

of 24h, we replaced one of the two objects with a new one and calculated the performance in novel object recognition. Both female and male cKO mice had a significantly lower performance in novel object recognition when compared to the control littermate (Fig. 4e). Additional automatically annotated motion tracking analyses via DeepLabCut [39] revealed a general sex difference in the mouse positioning relative to the objects over time (Supplementary Fig. 10). We then tested the mice in the three-chamber sociability test and the light-dark box. The two genotypes did not show any difference in the preference towards a social target in the sociability test (Fig. 4f) and did not display any differences in the time spent in the lit compartment of the LD box (Fig. 4g). They also had an equal first latency to the dark compartment (Fig. 4h) and had a similar number of lit-dark compartment transitions in the LD test (Fig. 4i). As the last test, the mice were exposed to the two-way active avoidance test. As shown in Fig. 4j both control and cKO mice learned the task over time and increased progressively the number of conditioned responses (i.e. to avoid foot-shock upon a tone presentation), but with differences among sex and genotypes. These differences were demonstrated in a three-way ANOVA showing a significant interaction between the day of the test, the sex, and the genotype. To further explain the role of sex and the genotype in this aversive learning test, we separated the learning curves of the males (Fig. 4k) from the females (Fig. 4l). The female cKO mice were significantly worse on day 2 and needed more trials to learn the task compared to the control littermate mice. Furthermore, when looking at the daily learning curves we found additional differences. The performance of both male and female cKO mice was worst on the second day of the test (Supplementary Fig. 11) and they were thus slower in learning the task. Taken together these data demonstrate that loss of GR in OPCs in early life does not impact on anxiety-relevant behaviors. Specifically, it leads to deficits

in hippocampus-dependent learning and memory in adulthood, both in non-aversive task and aversive learning where mice were exposed to moderate stress activation of the HPA axis[40–43].

Discussion

We established here a novel physiological role of GR-signaling in OPCs during postnatal brain development. Specifically, our findings demonstrate that early postnatal deletion of the GR in OPCs influences the maturation of hippocampal OLs in adulthood, alters neuronal network excitability in response to a mild stressor, and affects aversive learning later in life. Collectively, our data highlight that constitutive expression of GR in OPCs is critical for maintaining a physiological OPCs-OLs ratio and for supporting hippocampal activity and ensuring cognitive function related to the hippocampus.

First, we demonstrated that the cKO of GR in postnatal OPCs alters the density of OLs in the adult hippocampus, without affecting the density and proliferation of OPCs (Fig. 1). Previous studies have examined the role of GCs on the proliferation-maturation dynamics of the OLs in murine models. For instance, the exposure to ELA, which activates the HPA axis and elicits an increase in GCs[24,44], leads to precocious OLs differentiation in pups, and is associated with a depletion of the OPCs pool in adult mice[22]. These finding have also been corroborated by post-mortem studies from human individuals with a history of childhood trauma[23]. In contrast, in our experimental design, mice were not exposed to stress, and we focused instead on the physiological function of GCs by conditionally deleting GRs in OPCs during the early postnatal period. Our data suggest that physiological GC levels are essential for proper maturation of OPCs into OLs. Furthermore, GCs appear to play a key role in coordinating the timing of differentiation, as previously shown *in vitro*, via signaling clocks in precursor cells during development[45]. In support of this role of GCs, a recent *in vitro* study has shown differences in OPC proliferation and differentiation in response to corticosterone treatment. However these findings are difficult to generalize as they

are strictly dependent on the genetic background of the cells and on the timing of the treatment[46]. It is also however possible that GR deletion does not directly affect the maturation rate of the OL lineage but instead reduces the survival of the newly matured OLs, contributing to the observed decrease in OL density.

Postnatal GC concentrations are tightly controlled to shield the developing brain from stress-induced GC surges, a phenomenon known as the stress hyporesponsive period, during which moderate stressful challenges fail to trigger a significant stress hormone response[4]. Our data highlight a critical role for GR signaling in OPCs during this postnatal period, when basal levels of GCs are extremely low. We conclude that postnatal OPCs depend on a delicate regulation of circulating GCs. Elevated levels of GCs, as observed during early ELA, may disrupt OL lineage dynamics, resulting in changes associated with negative health outcomes. Conversely, maintaining homeostatic levels of GCs is likely crucial for supporting proper oligodendrocyte lineage maturation.

Beyond the canonical role of OPCs in sustaining oligodendrogenesis and myelin formation, our data also revealed a sex-specific non-canonical, myelination-independent, role of GR in OPCs in modulating neuronal network excitability upon challenge. We demonstrated that acute application of the synthetic GC agonist, dexamethasone, increased extracellular recorded field excitatory postsynaptic potentials (fEPSPs) and the paired-pulse ratio (PPR) in control female mice, but not in cKO mice. These data raised two important new points: first, they revealed a clear sex-specific electrophysiological response under acute challenging conditions (i.e. *ex vivo* dexamethasone application), indicating that female mice might be more sensitive to slight increases in circulating stress hormone and potentially more responsive to HPA activity[47–50]. Second, GR in OPCs appears to be necessary to induce changes in

neuronal network excitability in response to a mild and/or acute stressor. It has been shown previously that GCs modulate learning and memory processes. GCs also modulate synaptic transmission by slowly enhancing the amplitude of miniature excitatory postsynaptic currents (mEPSCs)[51] and rapidly facilitating synaptic potentiation in the mouse hippocampal CA1 area[52]. However, these data were always obtained by patching neurons. Here, we have shown for the first time that a specific non-neuronal cell type is required for such excitability. Since the Schaffer collateral largely consists of thin unmyelinated axons[53,54], it is likely that the observed changes in network activity depend on the ability of OPCs to directly modulate neuronal function through a non-canonical, myelin-independent, mechanism. The research field is only beginning to uncover the various mechanisms by which OPCs might regulate neuronal function[17,55]. These mechanisms include, for instance, the direct release of neurotransmitters[16], the shedding of the NG2 ectopic domain[15], and more indirect regulation of neuronal circuit homeostasis through the interaction with other glia cells[17]. Given the relatively short timeline of the employed experimental approach, these findings suggest a direct OPC-neuron communication, conceivably involving GR-signaling in OPCs.

The sex- and brain region-specific alterations observed *ex vivo* in the GR cKO mice occurred coincidently with an impaired performance in the non-aversive memory test (NORT) and in an aversive learning paradigm (TWA), especially in female mice. In the NORT, mice are exposed to novelty, which can be arousing, but is unlikely to lead to substantial increase of circulating GC[56]. In the TWA, mice are exposed to a mild stressful situation which triggers the activation of the HPA axis[43]. It has previously been shown that fear conditioning induces OPCs to proliferate and differentiate into myelinating oligodendrocytes[57] and that myelin formation is necessary for remote fear

memory retrieval. Similar data were obtained for non-aversive learning, including motor learning or hippocampal-related learning and memory in the Morris water maze[58]. Clinical data also support the importance of experience-dependent myelin formation. Indeed, structural MRI studies have shown that white matter changes are required for the acquisition of both new motor and cognitive skills (e.g. learning to read, juggling, piano playing)[59–61]. Moreover, cognitive deficits have been associated with (dys)function of the oligodendrocyte lineage and alterations in myelin content and ultrastructure[50–52].

Our cKO mice, which have a reduced density of OLs, showed deficits in the NORT and were slower than the controls in learning the task in the TWA. However, opposite to what might be expected, the reduction of mature OLs did not directly associate with drastic changes in myelin content (Supplementary Fig. 6) and myelin-axon unit structures, as shown by comparable levels of the main myelin structural proteins PLP and MBP and by comparable length of the nodes of Ranvier and paranodes, respectively. This suggests that the extant OLs, despite being reduced in the cKO mice, may still be sufficient to myelinate hippocampal axons. It is also important to note that comparable levels of myelin proteins and unaltered myelin-axon unit structures do not rule out potential subtle alterations in internodal length and myelin ultrastructure. These changes could impair baseline cognitive performance, such as those observed in the NORT, and may also affect myelin plasticity, which are critical for learning and memory consolidation[57,58].

Glucocorticoids play a critical role in memory formation[37,62]: both memory-enhancing and -impairing effects have been reported[37,63]. Extending the classical view that GC exert their cognition-modulating effects exclusively by modulating neuronal function, a recent study showed that the astrocyte-specific ablation of GR led to impaired aversive

memory expression in two different paradigms of Pavlovian learning[64]. Thus, it is tempting to speculate that proper memory formation, initiated by the activation of the HPA axis, requires GR expression in OPCs. Specifically, GR-signaling in OPCs might regulate two distinct pathways, both crucial for different stages of learning and memory. The first pathway, consistent with our electrophysiology data, could involve a fast-acting, non-canonical mechanism that directly modulates brain circuits involved in the initial phase of memory encoding. The second pathway could consist of a slow-acting canonical and myelination-related mechanism. This process would unfold over weeks, promoting OPC differentiation into OLs, facilitating myelination, and supporting memory consolidation. In this scenario, the deletion of GR in OPCs would significantly impair memory formation, weakening the entire learning and memory process, from initial acquisition to consolidation[65,66].

In conclusion, our data demonstrate that GRs are essential from the very early stages of postnatal development to regulate OL differentiation. The absence of these receptors appears to prime hippocampal network excitability and impair learning abilities, particularly under mild stress. This phenomenon likely involves both canonical and non-canonical functions of OPCs. Future studies are needed to clarify the conditions regulating each of these functions, and how they orchestrate cognitive processes in response to environmental challenges.

Materials and Methods

A succinct description of the experimental procedures related to the main results is provided below. Comprehensive materials and methods descriptions, including methods related to supplementary results, are reported in the supplementary material.

Mice. NG2-CreER^{T2} male mice (B6.Cspg4$^{tm1.1(cre/ERT2)Fki}$)[67] were crossed with female Nr3c1$^{fl/fl}$ (B6.Cg-Nr3c1$^{tm1.1Jda/J}$, Jacksons Lab, #021021) to obtain NG2-CreER^{T2} x Nr3c1$^{fl/fl}$ mice (cKO mice), which expressed tamoxifen-dependent Cre recombinase under the control of the NG2 transcriptional regulatory elements and Nr3c1 gene flanked by two loxP sites. NG2-CreER^{T2} x Nr3c1$^{fl/fl}$ male mice were then bred with Nr3c1$^{fl/fl}$ female mice to obtain the experimental mice. Littermate Nr3c1$^{fl/fl}$ were employed as control (Ctrl). Tamoxifen (TAM, Sigma-Aldrich, T5648) was dissolved in pure ethanol (Laborchem® international, LC-8657.1) and diluted in corn oil (Sigma-Aldrich, C8267) at a working concentration of 20 mg ml^{-1}. All the pups included in the experiment received i.p. injection of 0.1mg tamoxifen in 5 µl vehicle at postnatal day 2 (P2) and P4[68]. The mice were allowed to reach adulthood undisturbed, except for the conventional caretaking routine procedure in the mouse unit. Genotyping was performed as described before[67] or adapted from the recommended protocol on the JAX datasheet via standard PCR of genomic DNA. Primer sequences are reported in the supplementary materials and representative genotyping output in Supplementary figure 2. All experiments were then conducted on adult mice of both sexes (8-12 weeks old). Mice of the same sex were grouped housed (3-5 per cage) and maintained at a 12/12h light-dark cycle (lights on at 7:00 A.M.), at controlled temperature and humidity (temperature = 22 ± 2 °C, relative humidity = 50 ± 5%). Food and water were available *ad libitum*. All experiments were performed in accordance with the European directive

2010/63/EU for animal experiments and were approved by the local authorities (Animal Protection Committee of the State Government, Landesuntersuchungsamt Rheinland-Pfalz, Koblenz, Germany).

Flow cytometry. Naïve mice were sacrificed with isoflurane (Piramal Critical Care Deutschland; Cat# 4150097146757) and perfused with ice-cold 0.1 M pH 7.4 phosphate buffer saline (PBS) (ThermoFisher Scientific, 10010023). The hippocampi and cortices were rapidly dissected and coarsely chopped in Hank's Balanced salt solution (HBSS + $CaCl_2$, $MgCl_2$) containing 1 mg/ml of papain (from papaya latex, dnase ISigma-Aldrich, 51807363), including 40 μg/ml of DNase I (grade II from bovine pancreas, Sigma-Aldrich, 10104159001 (51743558)). Tissue was dissociated using gentleMACS™ Octo Dissociator (Miltenyi) using a built-in ready-to-use program optimized for small quantities (<100 mg) of the CNS tissue. The cells were then resuspended in 8 ml DMEM/ 1% horse serum and filtered through 70-μm cell strainers. The resulting cell pellet was then re-suspended in 25% Percoll solution (Cytiva) and centrifuged (25 min, room temperature (RT), 300 × *g*). Cells were resuspended in MACS Neuro Medium (Miltenyi Biotec, 130-093-570) containing 1x MACS NeuroBrew-21 (Miltenyi, 130-093-566), 100 U/ml Penicillin Streptomycin (Thermo Fisher Scientific, 15140122) and 2 mM L-Glutamine (Thermo Fisher Scientific, 25030-024 (51709381), and incubated with slow rotation at 37 °C for two hours. After washing the cells in FACS buffer (0,5% bovine serum albumin (PAN-Biotech P06-1391500 (51809570)), 2 mM Ethylenediaminetetraacetic Acid (EDTA, Sigma-Aldrich) in PBS), Fc receptors were blocked for 10 min with Fc-block (1:100 in FACS buffer, BioXCell, BE0307). Surface antigens were then labelled for 20 min on ice with FACS buffer containing following reagents: 1:1000 Fixable Viability Dye eFluor™ 780 (eBioscience, 65-0865),

PE/Cyanine7 anti-mouse/human CD11b 1:1000 (BioLegend 101216), Brilliant Violet 510™ anti-mouse CD45 (BioLegend, 103138) and CD140a (PDGFRA) APC 1:10 (Miltenyi Biotec, 130-102-473). For intracellular staining cells were fixed and permeabilized with eBioscience™ Foxp3/transcription factor staining buffer set (ThermoFisher Scientific, 00552300) according to the manufacturer's instructions. Cells were analyzed by using a FACSCanto II device (BD Biosciences). Post-acquisition analysis was performed by using FlowJo software. A list of the employed antibodies is provided in the supplementary material.

Immunohistochemistry. Mice were anesthetized via i.p. of Ketamin/Xylaxin (200 mg/kg, 20 mg/kg) and intracardially perfused with ice-cold PBS followed by 4% paraformaldehyde (ChemCruz). Brains were post-fixed in 4% PFA at 4°C for 2 hours, with the exception for PDGFRA and Ki-67 staining and for Caspr and Nav1.6 (post-fixed 24 hours), then transferred into 30% sucrose in 0.1 M PBS, pH 7.4 for 48 h and afterwards embedded in a cryoprotective medium (Tissue-Tek, O.C.T., 4583, Sakura Finetek Europe). Free-floating coronal sections (30-35 µm) including the somatosensory cortex and dorsal hippocampus (bregma from -1.79mm to -2.53mm) were washed in PBS (3x20min), then incubated for 90 minutes in 0.5% (v/v) Triton X-100 in, followed by 1 hour of blocking and permeability with 10% goat or donkey serum in 0.5% Triton X-100 in PBS at RT. PDGFRA and Ki-67 immunostaining slices were permeabilized and blocked for 60 min and 150 minutes respectively. The sections were then incubated overnight (ON) at 4°C in primary antibody, diluted in 3% serum in 0.5% Triton X-100 in PBS. On the following day, sections were washed in PBS (3x20min) and incubated for 2 hours at RT with secondary antibody diluted in 3% serum in 0.5% Triton X-100 in PBS. The sections were then washed in PBS (3 x 20min),

counterstained with DAPI (1:10000 in ddH20, SIGMA, D9542) and mounted on SuperFrost slides (Epredia, K5800AMNZ72) with fluorescence mounting medium (Dako, S3023). For the paranodes and nodes of Ranvier immunohistochemistry, free-floating coronal sections (30-35 µm) including the somatosensory cortex and dorsal hippocampus (bregma from -1.79mm to -2.53mm) were washed in PBS (3x10min), blocked in 5%NGS, 2,5% BSA, 0,25% TritonX-100 in PBS for 1 hour at RT and incubated ON at 4°C in primary antibody diluted in 5%NGS, 2,5% BSA, 0,25% TritonX-100 in PBS. On the following day, sections were washed in PBS (4x10min) and incubated for 2 hours at RT with secondary antibody diluited in 5%NGS, 2,5% BSA, 0,25% TritonX-100 in PBS. The sections were then washed in PBS (4 x 10mi) and mounted mounted on slides wwith Vectashield plus DAPI (4',6-diamidino-2-phenylindole) mounting medium (#H-1200, Vector Laboratories). The used antibodies were: rabbit anti-Nav1.6 (1:250, #ASC-009, Alomone labs), mouse anti-CASPR (1:1000, #75-001, Neuromab), goat anti-rabbit Alexa Fluor 594 (1:500, 111-585-003, Jackson Immuno Research), donkey anti-mouse Alexa Fluor 488 (1: 500, 715-545-150, Jackson Immuno Research).A list of the employed antibodies is provided in the supplementary material. Naïve mice were employed for proliferation and PDGFRA+ cells density assessment and for the analysis of paranodes and nodes of Ranvier length; the remaining samples were collected from mice that underwent behavioral testing (see Fig. 1a).

Microscopy and image analysis. Images were acquired at a Leica TCS SP8 confocal laser scanning microscope. For cell quantification (density or percentage), confocal micrographs were acquired with a 20x/0.75 (HC PL APO IMM CORR CS2) or 40x/1.30 (HC PL APO OIL CS2) immersion objectives, at a format of 1024 × 1024 pixels. The

pinhole was set to 1 AU, the field of view ranged from 276.09 µm × 276.09 µm to 87.87 µm × 87.87 µm, and the voxel size from 270nm x 270nm x 1 µm (xyz) to 637nm x 637nm x 1 µm (xyz). For each mouse, 4-6 micrographs (2-3 brain sections) from the dorsal CA1 and L2/3 of the somatosensory cortex, were acquired and Z-stack images were processed and analyzed with ImageJ (NIH) software by a blinded experimenter[69]. Recombination efficiency was calculated as the proportion of AN2$^+$Olig2$^+$ cells co-expressing GR. Recombination specificity was estimated based on the proportion of neurons (NeuN$^+$), microglia (Iba1$^+$), astrocytes (GFAP$^+$), and the area covered by pericytes (PDGFRB$^+$) co-expressing GR. Cell density was calculated as the number of cells per unit area (cells/mm^2) by dividing the total cell count by the area of the region of interest (ROI). OPCs proliferation was calculated as the percentage of PDGFRA$^+$ cells co-expressing Ki-67$^+$. Only cells with a detectable DAPI signal were included in the analysis. For OPCs morphology analysis, confocal micrographs were acquired with a HC PL APO CS2 63x/1.40 oil objective; pinhole was set to 1AU, the image format to 1024 x 1024 pixel, the pixel size to 86nm x 86nm and the z-stack interval to 150nm. A detailed description of the workflow and analysis parameters are provided in the supplementary material. For the analysis of paranodes and nodes of Ranvier, imaging was performed with ZEISS LSM 880 Confocal Laser Scanning microscope with AiryScan (Zeiss). To image individual nodes within a field of view, a region around a node was cropped, and a z-stack of the cropped region was acquired. Z-stacks were acquired and pixel size set at 0.04 × 0.04 × 0.10 µm (x,y,z). For each mouse, 4-5 brain sections including CA1 region were analysed. An automated pipeline to segment and analyze the length of paranodes and nodes of Ranvier in the acquired 3D microscopy images was implemented [70].

Electrophysiological Recordings – Multielectrode Array.

Naïve mice of 9-12 weeks were used for electrophysiological experiments. After deep anaesthesia using i.p. injection of 200 mg/kg ketamine ketamine, choline-based artificial cerebrospinal fluid (c-ACSF) solution was perfused by injection into one heart ventricle, containing in mM: NaCl (87), KCl (2.5), $NaH_2PO4+H2O$ (1.25), choline chloride (37.5), NaHCO3 (25) and d-glucose (25), CaCl $*2H_2O$ (0.5), $MgCl_2$ (7) (pH of 7.4). The brain was removed and placed into ice-cold c-ACSF perfused with carbogen (95% oxygen and 5% carbon dioxide), then placed on a vibratome stage to cut horizontal slices with thickness of 350µm. Slices were collected in a storage chamber of normal ACSF, which contains (in mM) NaCl (125), KCl (3), MgSO4 x 7H2O (1.3), CaCl2 x H2O (2.5), NaH2PO4 x H2O (1.25), NaHCO3 (26) and d-glucose (13), to rest at room temperature for at least 40 minutes before use. On the multi-electrode array (MEA) chip (60MEA200/30iR; MEA2100 System, Multi Channel Systems MCS GmbH), the slice was constantly perfused with carbogenated normal ACSF, which also contained 0.01% EtOH in order to control for any ethanol-induced electrophysiological changes (see below). Each slice was precisely placed to position a stimulating electrode in the CA3 region and recording electrode in the CA1 region of the hippocampus, along the Schaffer Collateral pathway. A platinum grid was placed on top of the slice to ensure electrode-tissue contact before starting the recordings. All recording protocols were generated and applied by Multi Channel Experimenter 2.2 software. Spontaneous neuronal activity was measured by recording extracellular spike frequency whereby an event counted as a spike exceeding the downward threshold of five standard deviations from baseline activity. Events were recorded for 5 minutes and quantified by the Multi Channel Analyzer 2.2. For evoked activity, an input-output curve was generated by applying step-wise voltage stimulations that

ranged from 0.5V to 5V in 500mV steps. The maximum amplitude of each evoked field excitatory postsynaptic potential (fEPSP) was recorded by the electrode in the CA1 region for each slice. The paired-pulse stimulation protocol (PPR), which had a 50ms inter-stimulus interval, used the voltage stimulation intensity which produced an fEPSP equal to ~30% of the maximum evoked fEPSP amplitude from the input/output curve protocol, for each slice. After, the perfusion input was switched to carbogenated ACSF containing 200nM of Dexamethasone diluted in ethanol (0.01%). After wash-in of 30 minutes all protocols were repeated. On finishing, the slice was removed and the drug-infused ACSF completely washed out, before placing the next slice.

Behavioral testing. Mice were handled for 2 min daily for 3-5 days before the start of the testing. The latter was performed between 8:00 A.M and 2:00 P.M, in sound-attenuating boxes under consistent lighting conditions (37 lux), except for the light-dark box test all mice were randomized and experimenters were blinded during the tests. The behavioral tests were videotaped (Basler camera) and mouse performance automatically tracked with EthoVisionXT software 15.0 (Noldus). Manual scoring of the recorded behavior was performed by a blinded experiment using The Observer XT12 software (Noldus Information Technology). Behavioral tests (see paragraph below). The tests were performed in the following order: Open field test (OFT), Novel object recognition test (NORT), three-chambers social interaction test, Light-Dark (LD) Box Test, and Two-way active avoidance (TWA) test. Detailed descriptions of the protocols are provided in the supplementary information.

Statistical analysis.

The analyses were performed with GraphPad Prism software10.0 or with R software, version 4.4.2. Significance level was set to $P < 0.05$ and the data are presented as mean ± SEM. Sample distribution was assessed via Shapiro-Wilk normality test. For normally distributed dataset, two-group comparison was performed via unpaired or paired two-tailed t-test. For non-normally distributed dataset, two-group comparison was performed via Mann–Whitney U (unpaired data) or Wilcoxon test (paired data). Correlation was assessed via Pearson's or Spearman's (non-parametric) test. Comparison between more than two groups were carried out by, two-way or three-way ANOVA, followed by Tukey's or Sidak post-hoc test. Mixed model design was applied for the statistical comparison of the nodes of Ranvier between groups. The number of biological replicates (n), specific statistical tests, and their P-values are indicated in the figure legends. Behavioral experiments were replicated in two independent batches. Detailed information of the statistical analyses are provided in the supplementary tables file.

CRediT authorship contribution statement

Conceptualization: LM, MBM, GT

Data Curation: LM, GP, CG, KB, JE, MP, DH, LN, SW, HS, GT

Formal Analysis: LM, GP, CG, KB, JE, MP, SW, HS, GT

Funding Acquisition: BT, AW, TM, MS, MBM, GT

Investigation: LM, GP, CG, KB, MP, JE, MK, DH, LN, AC, SW, GT

Methodology: LM, GP, CG, KB, MP, JE, MK, AC, SW, GT

Project Administration: MBM, GT

Resources: MS, MBM, GT

Software: NA

Supervision: MS, MBM, GT

Validation: LM, GP, CG, KB, MP, JE, MK, SW, GT

Visualization: LM, GP, CG, KB, MP, SW, GT

Writing – Original Draft Preparation: LM, GP, CG, GT

Writing – Review & Editing: LM, GP, CG, KB, MP, JE, MK, DH, LN, AC, SW, BL, AW, IH, TM, MS, MBM, GT

Conflict of interest

The authors declare no conflict of interest.

Acknowledgment

This work was supported by Leibniz Competition funds (Leibniz ScienceCampus NanoBrain, W71/2022) and by the German Research Foundation (CRC 1080, C02 to T.M.). The authors acknowledge Dr. R. Piccinno, Dr. S. Ritz and the IMB Microscopy & Histology Core Facility for supporting with the image analysis workflow. We are very grateful Verena Opitz, Julia Deuster and Jennifer Klüpfel, for technical support during the experiments. We are grateful to Dr. Julia Leschik for helping to design the PCR primers. We are grateful to Dr. Konstantin Radyushkin, Dr. Ulrich Schmitt and the Mouse Behaviour Unit (MBU) of the Leibniz Institute for Resilience Research (LIR) for animal care and for supporting the animal experimental procedures. We are grateful to Prof. Jaqueline Trotter for the scientific discussion. The work

described herein was carried out in partial fulfilment of the requirements for a doctoral degree at the Johannes Gutenberg University Medical Center Mainz, Germany.

References

1. Petanjek, Z. *et al.* Extraordinary neoteny of synaptic spines in the human prefrontal cortex. *Proc. Natl. Acad. Sci.* **108**, 13281–13286 (2011).
2. Bick, J. & Nelson, C. A. Early Adverse Experiences and the Developing Brain. *Neuropsychopharmacology* **41**, 177–196 (2016).
3. LeMoult, J. *et al.* Meta-analysis: Exposure to Early Life Stress and Risk for Depression in Childhood and Adolescence. *J. Am. Acad. Child Adolesc. Psychiatry* **59**, 842–855 (2020).
4. Schmidt, M. V. *et al.* The postnatal development of the hypothalamic-pituitary-adrenal axis in the mouse. *Int. J. Dev. Neurosci. Off. J. Int. Soc. Dev. Neurosci.* **21**, 125–132 (2003).
5. Warhaftig, G., Almeida, D. & Turecki, G. Early life adversity across different cell- types in the brain. *Neurosci. Biobehav. Rev.* **148**, 105113 (2023).
6. Zhou, B., Zhu, Z., Ransom, B. R. & Tong, X. Oligodendrocyte lineage cells and depression. *Mol. Psychiatry* **26**, 103–117 (2021).
7. Nave, K.-A. & Ehrenreich, H. Myelination and Oligodendrocyte Functions in Psychiatric Diseases. *JAMA Psychiatry* **71**, 582 (2014).
8. Nagy, C. *et al.* Single-nucleus transcriptomics of the prefrontal cortex in major depressive disorder implicates oligodendrocyte precursor cells and excitatory neurons. *Nat. Neurosci.* **23**, 771–781 (2020).
9. Poggi, G., Wennström, M., Müller, M. B. & Treccani, G. NG2-glia: rising stars in stress-related mental disorders? *Mol. Psychiatry* **28**, 518–520 (2023).
10. Nishiyama, A., Komitova, M., Suzuki, R. & Zhu, X. Polydendrocytes (NG2 cells): multifunctional cells with lineage plasticity. *Nat. Rev. Neurosci.* **10**, 9–22 (2009).
11. Dimou, L. & Gallo, V. NG2-glia and their functions in the central nervous system. *Glia* **63**, 1429 (2015).
12. Hill, R. A. & Nishiyama, A. NG2 cells (polydendrocytes): Listeners to the neural network with diverse properties. *Glia* **62**, 1195–1210 (2014).

13. Hughes, E. G., Kang, S. H., Fukaya, M. & Bergles, D. E. Oligodendrocyte progenitors balance growth with self-repulsion to achieve homeostasis in the adult brain. *Nat. Neurosci.* **16**, 668–676 (2013).
14. Eugenín-von Bernhardi, J. & Dimou, L. NG2-glia, More Than Progenitor Cells. in *Glial Cells in Health and Disease of the CNS* (ed. Von Bernhardi, R.) vol. 949 27–45 (Springer International Publishing, Cham, 2016).
15. Sakry, D. *et al.* Oligodendrocyte Precursor Cells Modulate the Neuronal Network by Activity-Dependent Ectodomain Cleavage of Glial NG2. *PLoS Biol.* **12**, e1001993 (2014).
16. Zhang, X. *et al.* NG2 glia-derived GABA release tunes inhibitory synapses and contributes to stress-induced anxiety. *Nat. Commun.* **12**, 5740 (2021).
17. Buchanan, J., Costa, N. M. da & Cheadle, L. Emerging roles of oligodendrocyte precursor cells in neural circuit development and remodeling. *Trends Neurosci.* **46**, 628 (2023).
18. Xiao, Y. & Czopka, T. Myelination-independent functions of oligodendrocyte precursor cells in health and disease. *Nat. Neurosci.* **26**, 1663–1669 (2023).
19. Mount, C. W., Yalçın, B., Cunliffe-Koehler, K., Sundaresh, S. & Monje, M. Monosynaptic tracing maps brain-wide afferent oligodendrocyte precursor cell connectivity. *eLife* **8**, e49291 (2019).
20. Bergles, D. E., Jabs, R. & Steinhäuser, C. Neuron-glia synapses in the brain. *Brain Res. Rev.* **63**, 130–137 (2010).
21. Bergles, D. E., Roberts, J. D. B., Somogyi, P. & Jahr, C. E. Glutamatergic synapses on oligodendrocyte precursor cells in the hippocampus. *Nature* **405**, 187–191 (2000).
22. Teissier, A. *et al.* Early-life stress impairs postnatal oligodendrogenesis and adult emotional behaviour through activity-dependent mechanisms. *Mol. Psychiatry* **25**, 1159–1174 (2020).
23. Tanti, A. *et al.* Child abuse associates with an imbalance of oligodendrocyte-lineage cells in ventromedial prefrontal white matter. *Mol. Psychiatry* **23**, 2018–2028 (2018).

24. Treccani, G. *et al.* Early life adversity targets the transcriptional signature of hippocampal NG2+ glia and affects voltage gated sodium (Nav) channels properties. *Neurobiol. Stress* **15**, 100338 (2021).
25. Poggi, G., Albiez, J. & Pryce, C. R. Effects of chronic social stress on oligodendrocyte proliferation-maturation and myelin status in prefrontal cortex and amygdala in adult mice. *Neurobiol. Stress* **18**, 100451 (2022).
26. Kokkosis, A. G., Madeira, M. M., Mullahy, M. R. & Tsirka, S. E. Chronic stress disrupts the homeostasis and progeny progression of oligodendroglial lineage cells, associating immune oligodendrocytes with prefrontal cortex hypomyelination. *Mol. Psychiatry* **27**, 2833–2848 (2022).
27. Orso, R. *et al.* A systematic review and multilevel meta-analysis of the prenatal and early life stress effects on rodent microglia, astrocyte, and oligodendrocyte density and morphology. *Neurosci. Biobehav. Rev.* **150**, 105202 (2023).
28. Matsusue, Y., Horii-Hayashi, N., Kirita, T. & Nishi, M. Distribution of Corticosteroid Receptors in Mature Oligodendrocytes and Oligodendrocyte Progenitors of the Adult Mouse Brain. *J. Histochem. Cytochem.* **62**, 211–226 (2014).
29. Zhang, Y. *et al.* Purification and Characterization of Progenitor and Mature Human Astrocytes Reveals Transcriptional and Functional Differences with Mouse. *Neuron* **89**, 37–53 (2016).
30. Zhang, Y. *et al.* An RNA-Sequencing Transcriptome and Splicing Database of Glia, Neurons, and Vascular Cells of the Cerebral Cortex. *J. Neurosci.* **34**, 11929–11947 (2014).
31. Chetty, S. *et al.* Stress and glucocorticoids promote oligodendrogenesis in the adult hippocampus. *Mol. Psychiatry* **19**, 1275–1283 (2014).
32. Hill, R. A., Patel, K. D., Goncalves, C. M., Grutzendler, J. & Nishiyama, A. Modulation of oligodendrocyte generation during a critical temporal window after NG2 cell division. *Nat. Neurosci.* **17**, 1518–1527 (2014).

33. Boulanger, J. J. & Messier, C. Unbiased stereological analysis of the fate of oligodendrocyte progenitor cells in the adult mouse brain and effect of reference memory training. *Behav. Brain Res.* **329**, 127–139 (2017).

34. Krämer-Albers, E.-M., Gehrig-Burger, K., Thiele, C., Trotter, J. & Nave, K.-A. Perturbed Interactions of Mutant Proteolipid Protein/DM20 with Cholesterol and Lipid Rafts in Oligodendroglia: Implications for Dysmyelination in Spastic Paraplegia. *J. Neurosci.* **26**, 11743–11752 (2006).

35. Wang, J. H. & Kelly, P. T. Attenuation of paired-pulse facilitation associated with synaptic potentiation mediated by postsynaptic mechanisms. *J. Neurophysiol.* **78**, 2707–2716 (1997).

36. Wang, J. H. & Kelly, P. T. Regulation of synaptic facilitation by postsynaptic Ca2+/CaM pathways in hippocampal CA1 neurons. *J. Neurophysiol.* **76**, 276–286 (1996).

37. de Quervain, D., Schwabe, L. & Roozendaal, B. Stress, glucocorticoids and memory: implications for treating fear-related disorders. *Nat. Rev. Neurosci.* **18**, 7–19 (2017).

38. Zucker, R. S. Short-Term Synaptic Plasticity. *Annu. Rev. Neurosci.* **12**, 13–31 (1989).

39. Mathis, A. *et al.* DeepLabCut: markerless pose estimation of user-defined body parts with deep learning. *Nat. Neurosci.* **21**, 1281–1289 (2018).

40. Piazza, P. V. *et al.* Corticosterone levels determine individual vulnerability to amphetamine self-administration. *Proc. Natl. Acad. Sci.* **88**, 2088–2092 (1991).

41. Bevins, R. A. *et al.* Novel-object place conditioning: behavioral and dopaminergic processes in expression of novelty reward. *Behav. Brain Res.* **129**, 41–50 (2002).

42. Antunes, M. & Biala, G. The novel object recognition memory: neurobiology, test procedure, and its modifications. *Cogn. Process.* **13**, 93–110 (2012).

43. Lucas, M., Chen, A. & Richter-Levin, G. Hypothalamic Corticotropin-Releasing Factor is Centrally Involved in Learning Under Moderate Stress. *Neuropsychopharmacology* **38**, 1825–1832 (2013).

44. Rice, C. J., Sandman, C. A., Lenjavi, M. R. & Baram, T. Z. A Novel Mouse Model for Acute and Long-Lasting Consequences of Early Life Stress. *Endocrinology* **149**, 4892–4900 (2008).
45. Barres, A., Lazar, M. A. & Raff, M. C. A novel role for thyroid hormone, glucocorticoids and retinoic acid in timing oligodendrocyte development. *Development* **120**, 1097–1108 (1994).
46. Gigliotta, A. *et al.* Genetic background modulates the effect of glucocorticoids on proliferation, differentiation and myelin formation of oligodendrocyte lineage cells. *Eur. J. Neurosci.* **59**, 2276–2292 (2024).
47. Albert, K. M. & Newhouse, P. A. Estrogen, Stress, and Depression: Cognitive and Biological Interactions. *Annu. Rev. Clin. Psychol.* **15**, 399 (2019).
48. Wang, J. *et al.* Gender difference in neural response to psychological stress. *Soc. Cogn. Affect. Neurosci.* **2**, 227–239 (2007).
49. Oakley, R. H., Riddick, N. V., Moy, S. S. & Cidlowski, J. A. Imbalanced glucocorticoid and mineralocorticoid stress hormone receptor function has sex-dependent and independent regulatory effects in the mouse hippocampus. *Neurobiol. Stress* **28**, 100589 (2024).
50. Kroon, J., Pereira, A. M. & Meijer, O. C. Glucocorticoid Sexual Dimorphism in Metabolism: Dissecting the Role of Sex Hormones. *Trends Endocrinol. Metab.* **31**, 357–367 (2020).
51. Karst, H. & Joëls, M. Corticosterone slowly enhances miniature excitatory postsynaptic current amplitude in mice CA1 hippocampal cells. *J. Neurophysiol.* **94**, 3479–3486 (2005).
52. Wiegert, O., Joëls, M. & Krugers, H. Timing is essential for rapid effects of corticosterone on synaptic potentiation in the mouse hippocampus. *Learn. Mem. Cold Spring Harb. N* **13**, 110–113 (2006).
53. Shepherd, G. M. G. & Harris, K. M. Three-Dimensional Structure and Composition of CA3→CA1 Axons in Rat Hippocampal Slices: Implications for Presynaptic Connectivity and Compartmentalization. *J. Neurosci.* **18**, 8300–8310 (1998).
54. Boiko, T. *et al.* Compact Myelin Dictates the Differential Targeting of Two Sodium Channel Isoforms in the Same Axon. *Neuron* **30**, 91–104 (2001).

55. Fang, L.-P. & Bai, X. Oligodendrocyte precursor cells: the multitaskers in the brain. *Pflüg. Arch. - Eur. J. Physiol.* **475**, 1035–1044 (2023).
56. Okuda, S., Roozendaal, B. & McGaugh, J. L. Glucocorticoid effects on object recognition memory require training-associated emotional arousal. *Proc. Natl. Acad. Sci.* **101**, 853–858 (2004).
57. Pan, S., Mayoral, S. R., Choi, H. S., Chan, J. R. & Kheirbek, M. A. Preservation of a remote fear memory requires new myelin formation. *Nat. Neurosci.* **23**, 487–499 (2020).
58. Steadman, P. E. *et al.* Disruption of Oligodendrogenesis Impairs Memory Consolidation in Adult Mice. *Neuron* **105**, 150-164.e6 (2020).
59. Scholz, J., Klein, M. C., Behrens, T. E. J. & Johansen-Berg, H. Training induces changes in white-matter architecture. *Nat. Neurosci.* **12**, 1370–1371 (2009).
60. Bonetto, G., Belin, D. & Káradóttir, R. T. Myelin: A gatekeeper of activity-dependent circuit plasticity? *Science* **374**, eaba6905 (2021).
61. Fields, R. D. Myelination: An Overlooked Mechanism of Synaptic Plasticity? *The Neuroscientist* **11**, 528–531 (2005).
62. Schwabe, L., Hermans, E. J., Joëls, M. & Roozendaal, B. Mechanisms of memory under stress. *Neuron* **110**, 1450–1467 (2022).
63. Schwabe, L., Joëls, M., Roozendaal, B., Wolf, O. T. & Oitzl, M. S. Stress effects on memory: an update and integration. *Neurosci. Biobehav. Rev.* **36**, 1740–1749 (2012).
64. Tertil, M. *et al.* Glucocorticoid receptor signaling in astrocytes is required for aversive memory formation. *Transl. Psychiatry* **8**, 1–11 (2018).
65. Fields, R. D. & Bukalo, O. Myelin makes memories. *Nat. Neurosci.* **23**, 469–470 (2020).
66. Xin, W. & Chan, J. R. Myelin plasticity: sculpting circuits in learning and memory. *Nat. Rev. Neurosci.* **21**, 682–694 (2020).
67. Huang, W. *et al.* Novel NG2-CreERT2 knock-in mice demonstrate heterogeneous differentiation potential of NG2 glia during development. *Glia* **62**, 896–913 (2014).
68. Masuda, T. *et al.* Author Correction: Novel Hexb-based tools for studying microglia in the CNS. *Nat. Immunol.* **21**, 1302–1302 (2020).

69. Schindelin, J. *et al.* Fiji: an open-source platform for biological-image analysis. *Nat. Methods* **9**, 676–682 (2012).

70. Koskinen, M.-K. *et al.* Node of Ranvier remodeling in chronic psychosocial stress and anxiety. *Neuropsychopharmacol. Off. Publ. Am. Coll. Neuropsychopharmacol.* **48**, 1532–1540 (2023).

Figure and figure legend

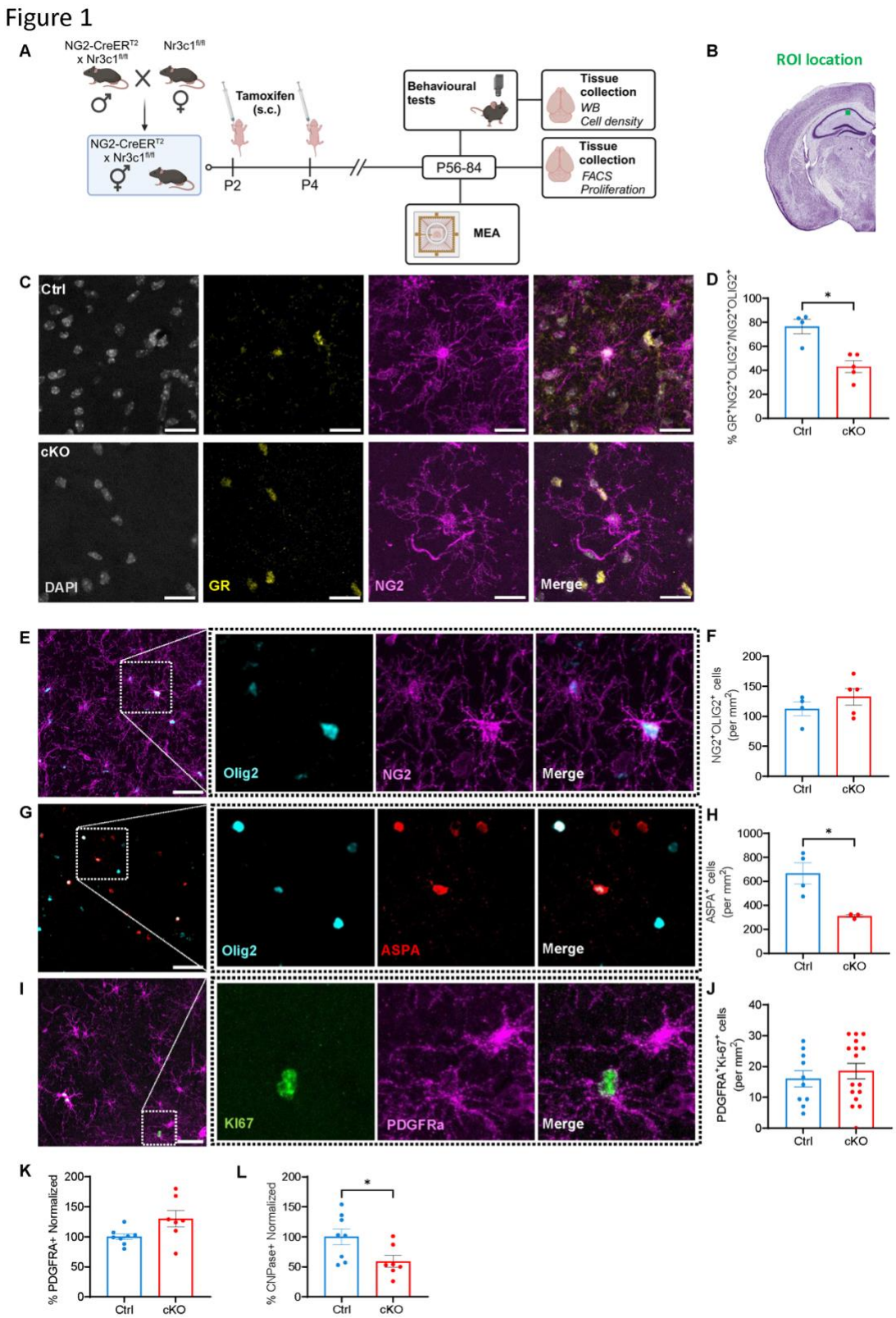

Figure 1. OPCs-specific GR cKO alter oligodendrocyte density but does not

induce changes in OPC density and proliferation. (**a**) Breeding strategy and experimental timeline for tamoxifen injections, behavioral studies, MEA recordings, and immunohistochemical analysis. (**b**) Region of interest (ROI, Cornu ammonis 1 (CA1), Bregma: -1.79 to -2.53 mm, image adapted from Paxinos and Franklin mouse brain atlas). (**c-j**) **Immunofluorescence in hippocampus**. (**c**) Representative confocal images of the co-expression of GR (yellow) and NG2 (magenta) in the hippocampus of Ctrl and cKO mice. Scale bar = 20 μm (**d**) Percentage of GR+NG2+ cells (Mann Whitney test: U = 0, p = 0.0159; n = 4 Ctrl and n = 5 cKO mice). Representative confocal images with digital magnification of the boxed area and related quantification for (**e-f**) NG2 (magenta) and (**g-h**) ASPA (red), each co-stained with Olig2 (cyan). Scale bar = 20 μm. (**f**) Density of NG2+Olig2+ cells (unpaired t test: p = 0.3202; n = 4 Ctrl and n = 5 cKO mice). (**h**) Density of ASPA+ cells (unpaired t test with Welch's correction: t(3.129) = 4.038, p = 0.0252; n = 4 Ctrl and n = 5 cKO mice). (**i**) Representative confocal images with digital magnification of the boxed area and related quantification for PDGRFA + (magenta) and Ki-67+ (green) cells. Scale bar = 20 μm. (**j**) Density of PDGRFA +Ki67+ cells (unpaired t test: p = 0.5153; n = 10 Ctrl and n = 16 cKO mice). Brightness and contrast of the micrographs have been adjusted for display purposes. (**k-l**) **Flow cytometry in hippocampal tissue.** (**k**) Percentage of PDGRFA+ cell in the CD1145-CD11b- population (unpaired t test with Welch's correction: p = 0.073; n = 8 Ctrl and n = 7 cKO mice). (**l**) Percentage of CNPase+ cells in the CD1145-CD11b- population (unpaired t test: t(13) = 2.384, p = 0.0331; n = 8 Ctrl and n = 7 cKO mice). Data are expressed as the mean ± S.E.M and each dot represents one animal. *P < 0.05.

Figure 2

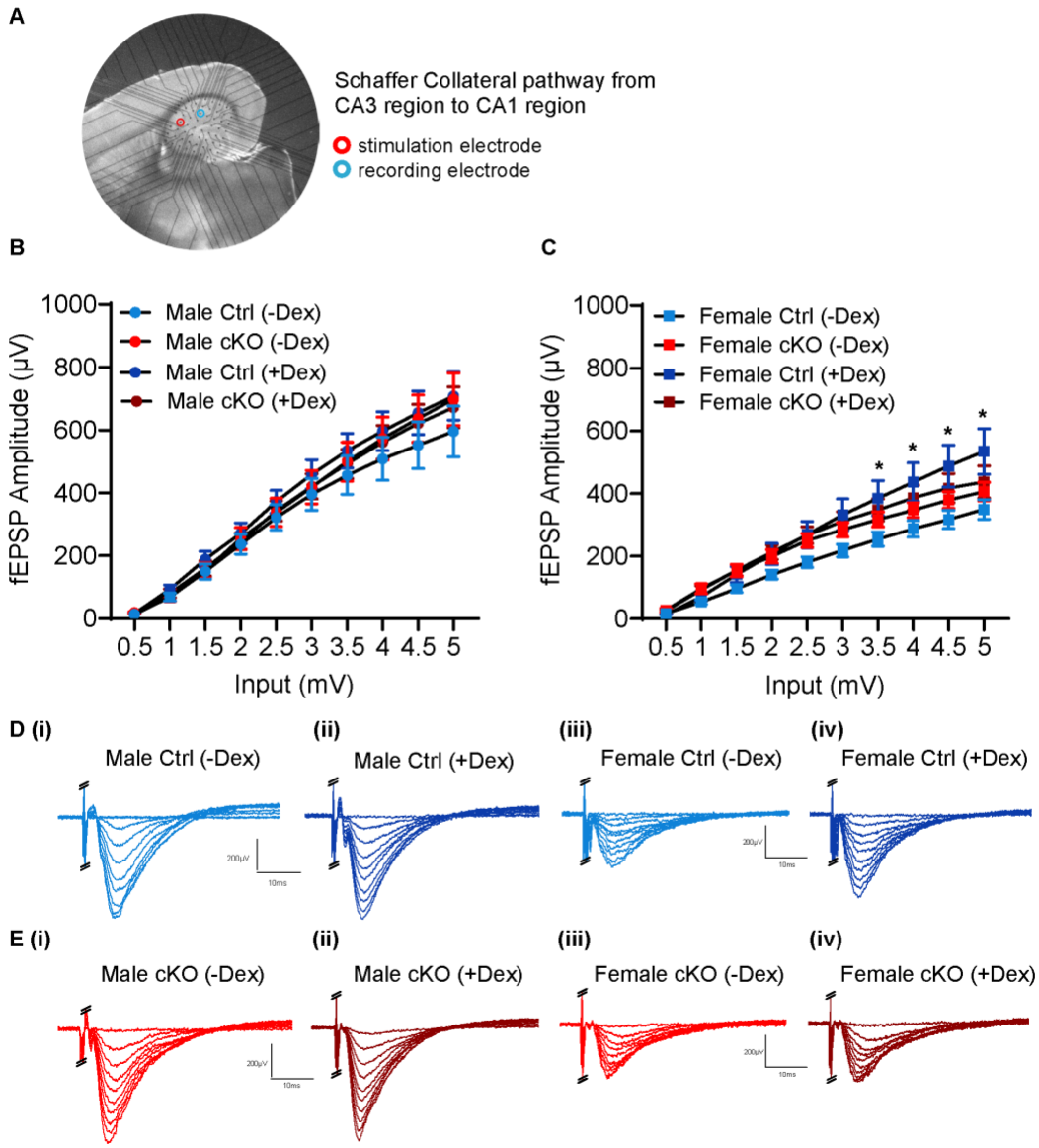

Figure 2. OPCs-specific GR affects hippocampal network excitability in the context of acute stress selectively in adult female mice. (**a**) Representative hippocampal brain section on MEA chip positioned with the stimulating electrode below the Schaffer Collaterals in area CA3 and the recording electrode below area CA1. (**b**) Evoked fEPSPs in the CA1 region of adult male wildtype and cKO mice before (light

blue/red, respectively) and 30 minutes after (dark blue/red, respectively) bath application of dexamethasone (Three-Way ANOVA: input, $F(9.000, 342.0) = 166.0$, $p < 0.0001$; n = 18 WT(-Dex), n = 22 cKO (-Dex), n = 18 WT (+Dex), n = 22 KO (+Dex)). (**c**) Evoked fEPSPs in the CA1 region of adult female wildtype and cKO mice before (light blue/red, respectively) and 30 minutes after (dark blue/red, respectively) bath application of dexamethasone (***Overall model, male***. Three-Way ANOVA: Input, $F(9.000, 342.0) = 166.0$, $p < 0.0001$; Dex, Genotype and Interaction, $p \geq 0.1725$. ***Overall model, female***. Three-Way ANOVA: Input x Genotype x Dex, $F(9, 278) = 3.622$, $p = 0.0003$; ***Statistical analysis per genotype – Female, Ctrl.*** Mixed-effects model: Input x Dex, $F(1.128, 16.80) = 5.702$. Paired t test as post-hoc comparison: input 3.5: (-Dex) < (+Dex), $p = 0.0406$; input 4: (-Dex) < (+Dex), $p = 0.0329$; input 4.5: (-Dex) < (+Dex), $p = 0.0249$; input 5: (-Dex) < (+Dex), $p = 0.0238$; n = 17 (-Dex), n = 16 (+Dex). ***Statistical analysis per genotype – Female, cKO.*** Two-way RM ANOVA, Input, $F(1.402, 22.43) = 90.15$, $p < 0.0001$; Dex and interaction, $p \geq 0.2581$; n = 17 (-Dex), n = 17 (+Dex)). (**d**) Representative overlaid voltage traces of the evoked I/O responses from male wildtype mice before (**i**) and after (**ii**) dexamethasone application, and female wildtype mice before (**iii**) and after (**iv**) dexamethasone application. (**e**) Representative overlaid voltage traces of the evoked I/O responses from male cKO mice before (**i**) and after (**ii**) dexamethasone application, and female cKO mice before (**iii**) and after (**iv**) dexamethasone application. Data are expressed as the mean ± S.E.M. * $p < 0.05$.

Figure 3

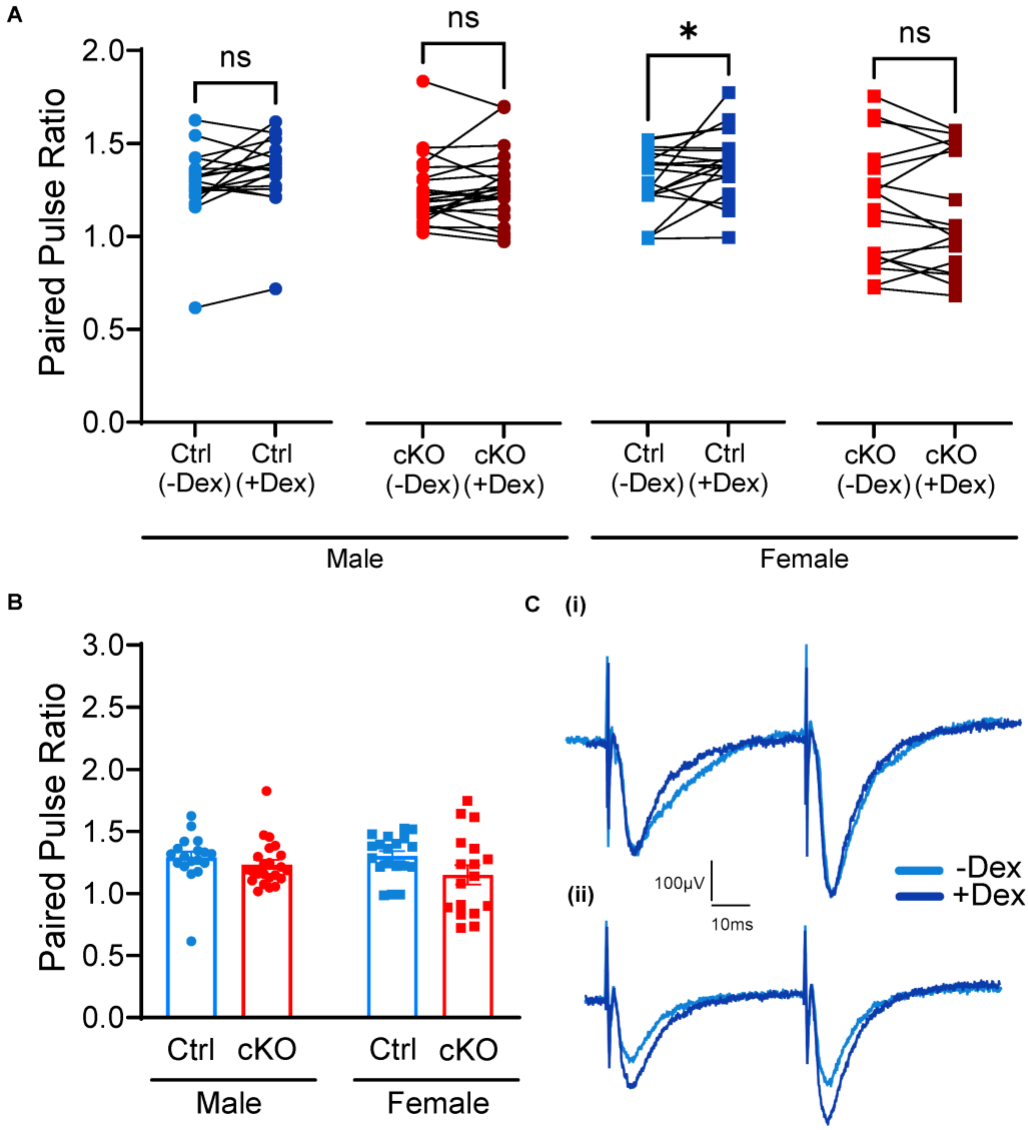

Figure 3. Sex-specific changes in synaptic short-term plasticity induced by acute stress in adult female mice depends on OPCspecific GRs. (a) Electrophysiological recordings of the paired-pulse ratios (PPR) in male Ctrl and cKO, female Ctrl and cKO, before and after 30-minute dexamethasone application (**Female, Ctrl**. Paired t test: t(18) = 2.247, p = 0.0374; n = 19 (-Dex), n = 19 (+Dex).

Female, cKO. Wilcoxon matched-pairs signed rank test: $W = -31.00$, $p = 0.4874$; $n = 17$ (-Dex), $n = 17$ (+Dex)). **(b)** Baseline paired pulse ratio (Two-way ANOVA: genotype, $F(1, 73) = 3.934$, $p = 0.0511$; sex and interaction, $p \geq 0.3529$). **(c) (i)** Representative trace of male Ctrl paired-pulse stimulation responses before (light blue) and after (dark blue) dexamethasone application. **(ii)** Representative trace of female Ctrl paired-pulse stimulation responses before (light blue) and after (dark blue) dexamethasone application. Data are expressed as the mean ± S.E.M. * $p < 0.05$.

Figure 4

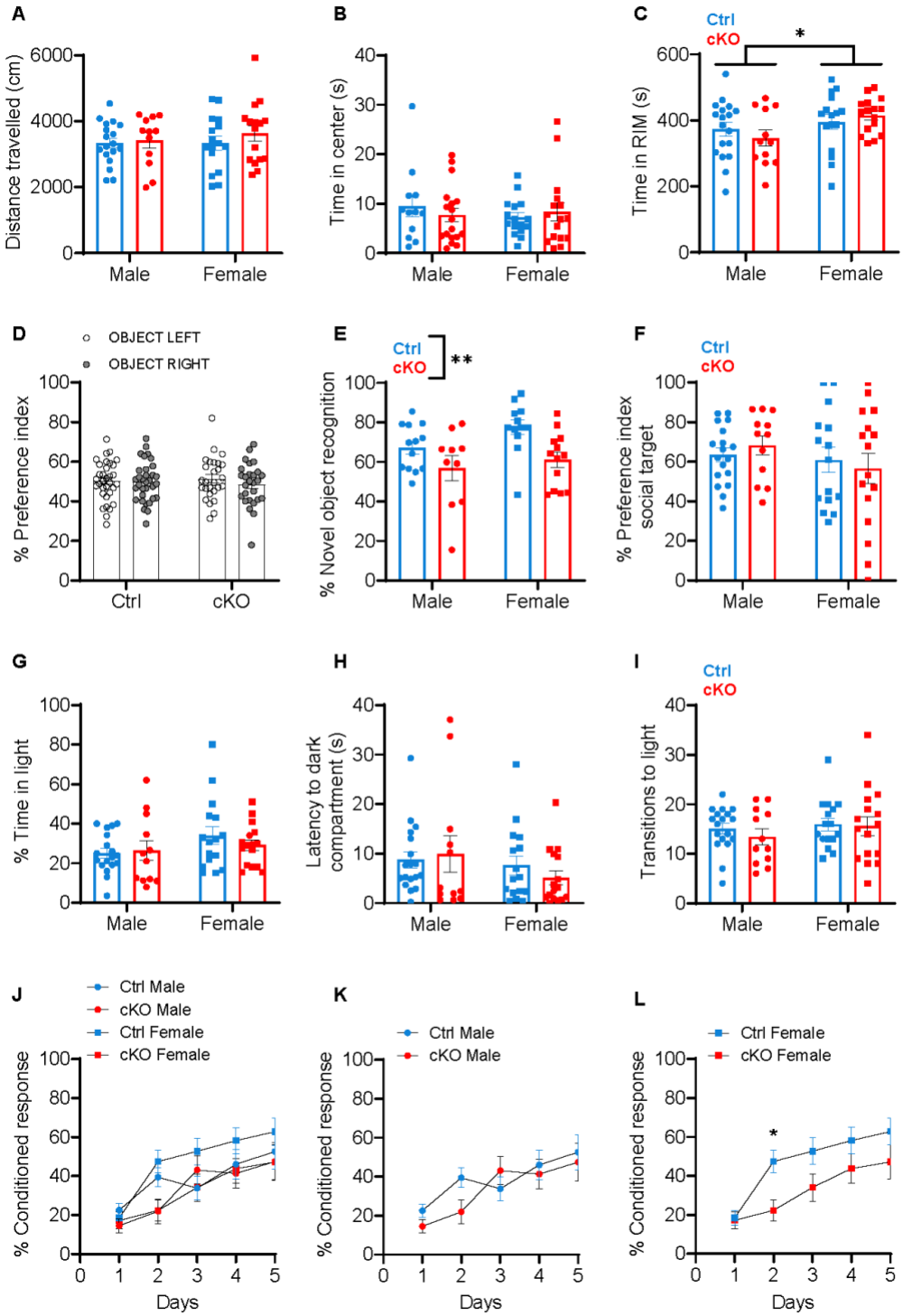

Figure 4. GR deletion in OPCs induces impairment in memory and aversive learning tasks. (**A-C**) **Open Field Test.** (**a**) Distance travelled (Two-way ANOVA: p≥ 0.2718). (**b**) Time spent in the center (Two-way ANOVA: p≥ 0.605). (**c**) Time spent in

the RIM (Two-way ANOVA: sex, $F(1, 58) = 4.707$, $p = 0.0342$; n = 18F/16F Ctrl and n = 12M/16F cKO). (**d-e**) **Novel object recognition test.** (**d**) Preference index (%) for two identical objects (Two-way ANOVA: $p = 0.3910$), and (**e**) novel object recognition (%) (Two-way ANOVA: genotype, $F(1, 44) = 10.02$, $p = 0.0028$; n = 13M/12F Ctrl and n = 10M/13F cKO). (**f**) Sociability index (Two-way ANOVA: $p \geq 0.229$; n = 18M/16F Ctrl and n = 12M/16F cKO). (**g-i**) **Light-Dark Box Test.** (**g**) Time spent in the lit compartment (Two-way ANOVA: $p \geq 0.1177$). (**h**) Latency to enter the dark compartment (Two-way ANOVA: $p \geq 0.1677$). (**i**) Frequency of light-dark transitions (Two-way ANOVA: $p \geq 0.3087$; n = 18M/16F Ctrl and n = 12M/16F cKO). (**j-l**) **Two-way active avoidance test.** (**j**) Percentage of conditioned response (CR) over days in both sexes (Three-way ANOVA: genotype x day x sex, $F (4, 224) = 2.555$, $p = 0.0398$; n = 17M/16F Ctrl and n = 12M/15F cKO). (**k**) Percentage of conditioned response (CR) over days in males (Two-way RM ANOVA: days x genotype, $F(4, 108) = 2.664$, $p = 0.0363$; Šídák's multiple comparisons test: *day 2: cKO = Ctrl*). (**l**) Percentage of conditioned response (CR) over days in females (Two-way RM ANOVA: days x genotype, $F(4, 116) = 3.010$, $p = 0.021$; Šídák's multiple comparisons test: *day 2: cKO < Ctrl, p = 0.0339*; n = 17M/16F Ctrl and n = 12M/15F cKO. Data are expressed as the mean ± S.E.M. *P < 0.05, **P < 0.01.